Proceedings of the 7th International Conference on Mechanics and Materials in Design
Albufeira/Portugal 11-15 June 2017. Editors J.F. Silva Gomes and S.A. Meguid.
Publ. INEGI/FEUP (2017)

PAPER REF: 6786

MODELLING OF CABLES AND FIBRES IN MULTIBODY DYNAMICS

Pavel Polach[1(*)], Jan Dupal[2], Zbyněk Šika[3], Michal Hajžman[2]
[1]Research and Testing Institute Plzeň, Plzeň, Czech Republic
[2]New Technologies for the Information Society, University of West Bohemia, Plzeň, Czech Republic
[3]Dep. of Mechanics, Biomechanics and Mechatronics, Czech Tech. Univ. in Prague, Prague, Czech Republic
[(*)]*Email:* polach@vzuplzen.cz

ABSTRACT

This paper summarizes the possible approaches suitable for the modelling of cable and fibre dynamics in the framework of various mechanical systems. Force representation of a cable, a point-mass model, an absolute nodal coordinate formulation and a general model based on Hamilton's principle are introduced. The QuadroSphere tilting mechanism with a spherical motion of a platform and an accurate measurement of its position is introduced.

Keywords: cable, multibody dynamics, nonlinear force, vibration

INTRODUCTION

Cables and fibres can play an important role in the design of many machines. One of the most interesting applications is the replacing of chosen rigid elements of a manipulator or a mechanism with cables. The main advantage of this design is achievement of a lower moving inertia, which leads to a higher mechanism speed, a large range of motion and the possibility of antibacklash property. The drawbacks can be related to the fact that cables should be only in tension in the course of a motion. This paper summarizes the possible approaches suitable to the modelling of cable dynamics in the framework of various mechanical systems.

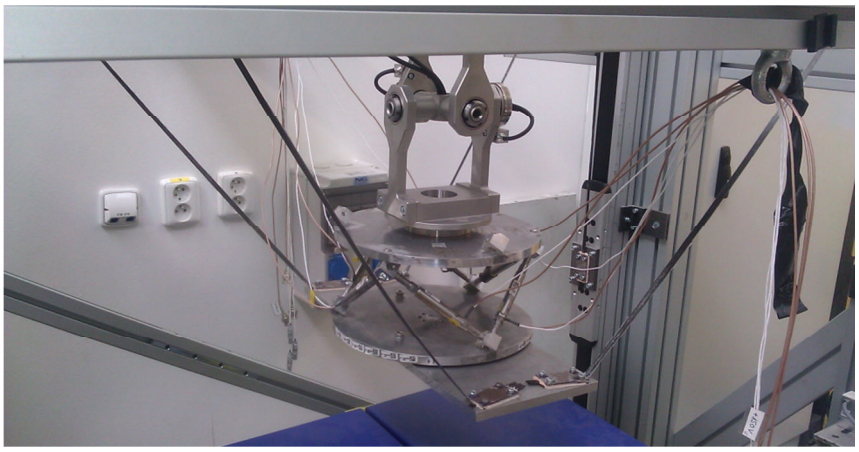

Fig. 1 - The QuadroSphere tilting mechanism

The motivation is the development of a cable model, which could be efficient for the usage in a mechatronic model of a manipulator consisting of cables and an end-effector whose motion is driven by cables - particularly for the usage in the model of QuadroSphere (see Fig. 1 and

Fig. 2; Polach, 2015a). The QuadroSphere is a tilting mechanism with a spherical motion of a platform and an accurate measurement of its position. The platform position is controlled by four fibres; each fibre is guided by a pulley from linear guidance to the platform. The numerical model of QuadroSphere will serve for the investigation of different possible strategies of the control of this active structure superimposed to the end-effector of the cable-driven mechanism in order to improve the end-effector positioning accuracy and the operational speed.

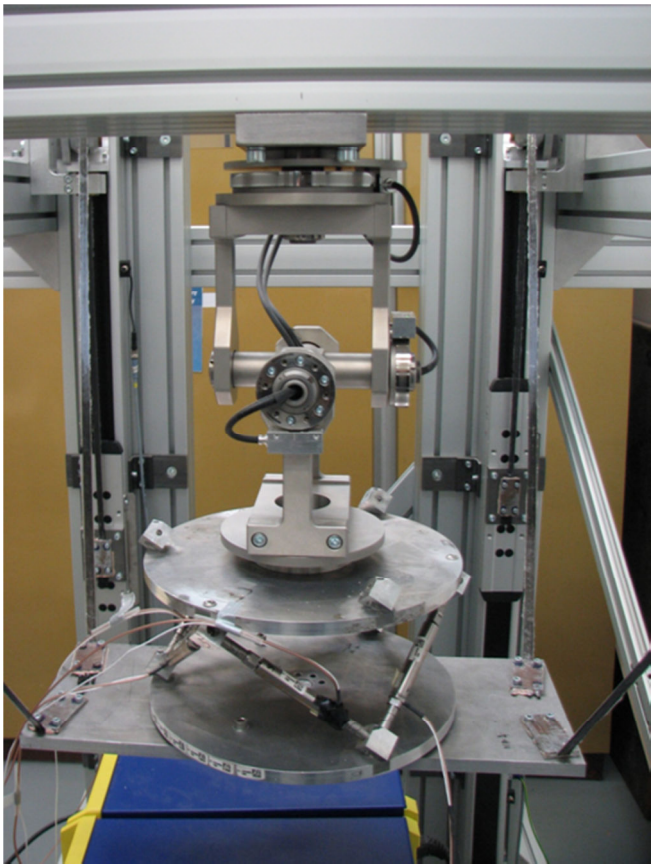

Fig. 2 - The QuadroSphere tilting mechanism

The cable (fibre, wire etc.) modelling (Hajžman, 2011) should be based on considering the cable flexibility and suitable approaches can be based on the flexible multibody dynamics (see e.g. Shabana, 1997; Lugrís, 2011; Gerstmayr, 2012).

Flexible multibody dynamics is a rapidly growing branch of computational mechanics and many industrial applications can be solved using newly proposed flexible multibody dynamics approaches. The studied problems are characterized by a general large motion of interconnected rigid and flexible bodies with the possible presence of various nonlinear forces and torques. There are many approaches to the modelling of flexible bodies in the framework of multibody systems (Hajžman, 2008). Comprehensive reviews of these approaches can be found in Shabana (1997) or in Wasfy (2003). Further development together with other multibody dynamics trends was introduced in Schiehlen (2007). Details of multibody formalisms and means of the creation of equations of motion can be found e.g. in Stejskal (1996), Awrejcewicz (2012).

The simplest way how to incorporate cables in the equations of motion of a mechanism is the force representation of a cable (e.g. Diao, 2009; Polach, 2015b). It is supposed that the mass

of cables is small to such an extent comparing to the other moving parts that the inertia of cables is negligible with respect to the other parts. The cable is represented by the force dependent on the cable deformation and its stiffness and damping properties. A variable length of the cable due to wiring can be easily described using the force approach. This way of the cable modelling is probably the most frequently used in the cable-driven robot dynamics and control (e.g. Heyden, 2006; Zi, 2008).

A more accurate approach is based on the representation of the cable using a point-mass model (e.g. Kamman, 2001; Polach, 2014; Ottaviano, 2015). It has the advantage of a lumped point-mass model. The point masses can be connected by forces or constraints. Wiring of a cable can be also simulated and a detailed model of a wiring mechanism can be observed. In the case of the manipulator mechatronic model consisting of cables and an end-effector whose motion is driven by cables (e.g. in the case of the QuadroSphere model - Polach, 2015a) utilization of the point-mass model of a cable proved to be very prospective.

In order to represent bending behaviour of cables their discretization using the finite segment method (Shabana, 1997) or so called rigid finite elements (Wittbrodt, 2006) is possible. Other more complex approaches can utilize nonlinear three-dimensional finite elements (Freire, 2006).

A very promising approach usable for the cable modelling is a so called absolute nodal coordinate formulation (ANCF), which is based on the discretization of a cable or a fibre to nonlinear finite elements (Shabana, 1997; Gerstmayr, 2012; Liu, 2012; Hajžman, 2015; Bulín, 2015; Bulín, 2017). Absolute nodal positions and slopes are considered to be nodal coordinates of the ANCF elements. The formulation leads to a constant mass matrix and highly nonlinear stiffness matrix. The model can be efficiently used for the investigation of various contact problems related to cables or fibres.

Another approach used for creation of a general model involving cables with distributed mass and time-varying length is based on Hamilton's principle, which serves to achieve a system of partial differential equations describing the cable dynamics (Du, 2015). To solve the system of dynamic equations, the Ritz-mode method with polynomial shape functions is employed and the system of partial differential equations is converted into ordinary differential equations. The accuracy of the cable model depends on the order of the used polynomial mode functions. This approach is suitable for the modelling of cable-driven manipulators with distributed mass flexible cables.

FORCE AND POINT-MASS REPRESENTATION OF THE CABLE

Model of the mechanical system with the end-effector attached to the frame using two cables is given as an example for introducing the force (see Fig. 3) and the point-mass (see Fig. 4) representation of the cable. The free length of the left cable is l_1, the free length of the right cable is l_2 and abbreviation EF denotes the end-effector (the weight) in Fig. 3 and Fig. 4.

The equation of motion of the system from Fig. 3 (force representation of the cable) can be written as a differential equation of the second order

$$m\,\ddot{\boldsymbol{r}} + b_1 \frac{\mathrm{d}\boldsymbol{l}_1}{\mathrm{d}t} + b_2 \frac{\mathrm{d}\boldsymbol{l}_2}{\mathrm{d}t} + k_1\,\mathrm{d}\boldsymbol{l}_1 + k_2\,\mathrm{d}\boldsymbol{l}_2 = \boldsymbol{f}\,, \tag{1}$$

where $\boldsymbol{r}$ is the position vector of the end-effector, $\ddot{\boldsymbol{r}}$ is the vector of acceleration of the end-effector, $\boldsymbol{r}_\mathrm{A}$ is the position vector of attachment of the left cable to the frame, $\boldsymbol{r}_\mathrm{B}$ is the position vector of attachment of the right cable to the frame, $\boldsymbol{r}_\mathrm{AEF} = \boldsymbol{r} - \boldsymbol{r}_\mathrm{A}$ is the vector from

point A (i.e. the attachment of the left cable to the frame) to the end-effector, $\boldsymbol{r}_{\mathrm{BEF}} = \boldsymbol{r} - \boldsymbol{r}_{\mathrm{B}}$ is the vector from point B (i.e. the attachment of the right cable to the frame) to the end-effector, $\mathrm{d}\boldsymbol{l}_1 = -\left(\left|\boldsymbol{r}_{\mathrm{AEF}}\right| - l_1\right)\dfrac{\boldsymbol{r}_{\mathrm{AEF}}}{\left|\boldsymbol{r}_{\mathrm{AEF}}\right|} H\left(\left|\boldsymbol{r}_{\mathrm{AEF}}\right| - l_1\right)$ is the vector of deformation of the left cable, $\left|\boldsymbol{r}_{\mathrm{AEF}}\right| = \sqrt{\boldsymbol{r}_{\mathrm{AEF}}^{\mathrm{T}}\,\boldsymbol{r}_{\mathrm{AEF}}}$, $\mathrm{d}\boldsymbol{l}_2 = -\left(\left|\boldsymbol{r}_{\mathrm{BEF}}\right| - l_1\right)\dfrac{\boldsymbol{r}_{\mathrm{BEF}}}{\left|\boldsymbol{r}_{\mathrm{BEF}}\right|} H\left(\left|\boldsymbol{r}_{\mathrm{BEF}}\right| - l_2\right)$ is the vector of deformation of the right cable, $\left|\boldsymbol{r}_{\mathrm{BEF}}\right| = \sqrt{\boldsymbol{r}_{\mathrm{BEF}}^{\mathrm{T}}\,\boldsymbol{r}_{\mathrm{BEF}}}$, $H(\ )$ is the Heaviside's step function, $\boldsymbol{f}$ is the vector of force acting on the end-effector, t is time, m is the mass of the end-effector, k_1 is the stiffness of the left cable, k_2 is the stiffness of the right cable, b_1 is the damping coefficient of the left cable and b_2 is the damping coefficient of the right cable.

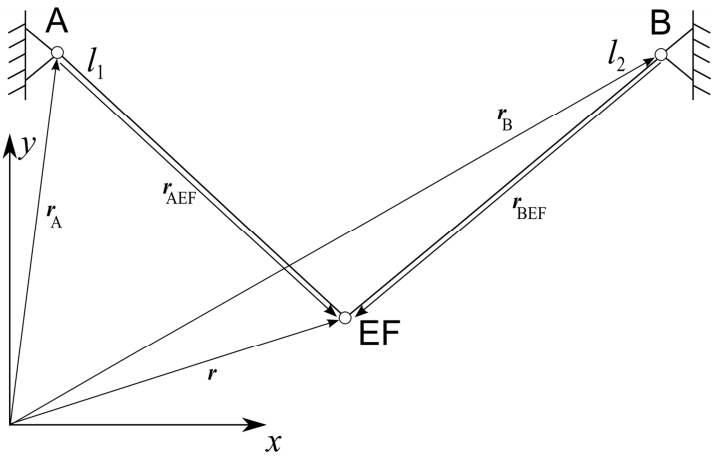

Fig. 3 - Model of the mechanical system with the end-effector attached to the frame using two cables with the force representation of the cable (in absolute coordinate system)

For each node of the system from Fig. 4 (point-mass representation of the cable) the following equation of motion can be written

$$m_i\,\ddot{\boldsymbol{r}}_i + b_i\,\frac{\mathrm{d}\boldsymbol{l}_i}{\mathrm{d}t} + b_{i+1}\,\frac{\mathrm{d}\boldsymbol{l}_{i+1}}{\mathrm{d}t} + k_i\,\mathrm{d}\boldsymbol{l}_i + k_{i+1}\,\mathrm{d}\boldsymbol{l}_{i+1} = \boldsymbol{f}_i\,, \tag{2}$$

where $\boldsymbol{r}_i$ is the position vector of node i (or end-effector), $\ddot{\boldsymbol{r}}_i$ is the vector of acceleration vector of node i, $\boldsymbol{r}_{i\text{-}1}$ is the position vector of node i-1, $\boldsymbol{r}_{i+1}$ is the position vector of node i+1, $\boldsymbol{r}_{i,\,i-1} = \boldsymbol{r}_i - \boldsymbol{r}_{i-1}$ is the vector from node i-1 to node i, $\boldsymbol{r}_{i,\,i+1} = \boldsymbol{r}_i - \boldsymbol{r}_{i+1}$ is the vector from node i+1 to node i, l_i is the free length of the part of the cable between node i-1 and node i, l_{i+1} is the free length of the part of the cable between node i and node i+1, $\mathrm{d}\boldsymbol{l}_i = -\left(\left|\boldsymbol{r}_{i,\,i-1}\right| - l_i\right)\dfrac{\boldsymbol{r}_{i,\,i-1}}{\left|\boldsymbol{r}_{i,\,i-1}\right|} H\left(\left|\boldsymbol{r}_{i,\,i-1}\right| - l_i\right)$ is the vector of deformation of the part of the cable between node i-1 and node i, $\left|\boldsymbol{r}_{i,\,i-1}\right| = \sqrt{\boldsymbol{r}_{i,\,i-1}^{\mathrm{T}}\,\boldsymbol{r}_{i,\,i-1}}$, $\mathrm{d}\boldsymbol{l}_{i+1} = -\left(\left|\boldsymbol{r}_{i,\,i+1}\right| - l_{i+1}\right)\dfrac{\boldsymbol{r}_{i,\,i+1}}{\left|\boldsymbol{r}_{i,\,i+1}\right|} H\left(\left|\boldsymbol{r}_{i,\,i+1}\right| - l_{i+1}\right)$ is the vector of deformation of the part of the cable between node i and node i+1,

$\left|\boldsymbol{r}_{i,\,i+1}\right| = \sqrt{\boldsymbol{r}_{i,\,i+1}^{\mathrm{T}}\,\boldsymbol{r}_{i,\,i+1}}$, $\boldsymbol{f}_i$ is the vector of force acting on node i, m_i is the mass of node i, k_i is the stiffness of the part of the cable between node i-1 and node i, k_{i+1} is the stiffness of the part of the cable between the node i and node i+1, b_i is the damping coefficient of the part of the cable between node i-1 and node i, b_{i+1} is damping coefficient of the part of the cable between node i and node i+1.

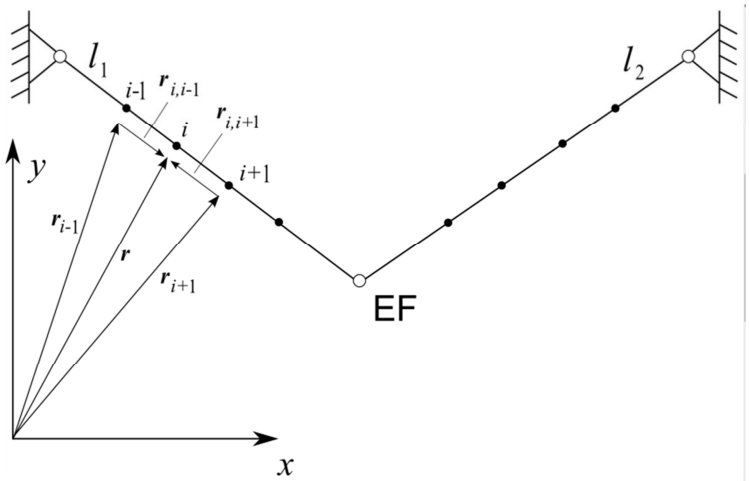

Fig. 4 - Model of the mechanical system with the end-effector attached to the frame using two cables with point-mass representation of the cable (in the absolute coordinate system)

Resultant equations of motion of all nodes and the end-effector lead to the system of differential equations of the second order in a matrix form.

ANCF CABLE MODEL

A planar ANCF beam element of length l with two nodes (see Fig. 5) is briefly introduced. Global position $\boldsymbol{r} = \left[r_x, r_y\right]^{\mathrm{T}}$ of an arbitrary beam point determined by parameter p can be written as

$$\boldsymbol{r}(p) = \boldsymbol{S}(p)\,\boldsymbol{e}\,, \quad \boldsymbol{e} = \left[e_1, e_2, \ldots, e_8\right]^{\mathrm{T}}, \tag{3}$$

where $\boldsymbol{S} \in \mathbf{R}^{2,8}$ is the global shape function matrix, $\boldsymbol{e}$ is the vector of element nodal coordinates and $p \in \langle 0, l \rangle$ is the parameter of a curve.

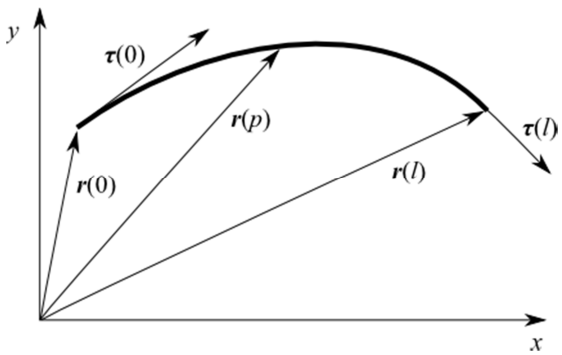

Fig. 5 - The planar ANCF beam element

Particular nodal coordinates in the case of cubic shape functions (Shabana, 2005) are

$$\begin{aligned} &e_1 = r_x(0), \quad e_2 = r_y(0), \quad e_3 = \tau_x(0) = \frac{\partial r_x(0)}{\partial p}, \quad e_4 = \tau_y(0) = \frac{\partial r_y(0)}{\partial p}, \\ &e_5 = r_x(l), \quad e_6 = r_y(l), \quad e_7 = \tau_x(l) = \frac{\partial r_x(l)}{\partial p}, \quad e_8 = \tau_y(l) = \frac{\partial r_y(l)}{\partial p}. \end{aligned} \tag{4}$$

The global shape function matrix in the case of the planar beam element is defined as

$$\begin{aligned} &\boldsymbol{S} = [s_1 \boldsymbol{I} \quad s_2 \boldsymbol{I} \quad s_3 \boldsymbol{I} \quad s_4 \boldsymbol{I}], \quad \boldsymbol{I} = \begin{bmatrix} 1 & 0 \\ 0 & 1 \end{bmatrix}, \\ &s_1 = 1 - 3\xi^2 + 2\xi^3, \quad s_2 = l\left(\xi - 2\xi^2 + \xi^3\right), \quad s_3 = 3\xi^2 - 2\xi^3, \quad s_4 = l\left(\xi^3 - \xi^2\right), \quad \xi = \frac{p}{l}. \end{aligned} \tag{5}$$

Standard procedures (e.g. the Lagrange equations or the principle of virtual work) can be used in order to derive a mathematical model of the planar ANCF beam element. Kinetic energy of the element of material density ρ is

$$E_k = \frac{1}{2}\int_0^l \rho A \dot{\boldsymbol{r}}^{\mathrm{T}} \dot{\boldsymbol{r}} \,\mathrm{d}p = \frac{1}{2}\dot{\boldsymbol{e}}^{\mathrm{T}} \int_0^l \rho A \boldsymbol{S}^{\mathrm{T}} \boldsymbol{S} \,\mathrm{d}p \, \dot{\boldsymbol{e}} = \frac{1}{2}\dot{\boldsymbol{e}}^{\mathrm{T}} \boldsymbol{M}_e \dot{\boldsymbol{e}}, \tag{6}$$

where $\boldsymbol{M}_e$ is the constant element mass matrix in the case of this formulation.

Strain energy E_p of the element is used for the derivation of elastic forces in the ANCF model and the form of an adopted elasticity model determines the complexity of the whole model. In Shabana (2005), there are several approaches, which employ the separation of strain energy of longitudinal deformation E_{pl} and strain energy of transverse (bending) deformation E_{pt} as

$$E_p = E_{pl} + E_{pt} = \frac{1}{2}\int_0^l E A \varepsilon_l^2 \,\mathrm{d}p + \frac{1}{2}\int_0^l E I \kappa^2 \,\mathrm{d}p, \tag{7}$$

where E is the Young modulus, A is the area of the cross-section and I is the second moment of the area about a transverse axis. The possible models are then classified according to the expressions for longitudinal strain ε_l and curvature κ. General expressions for these quantities are

$$\varepsilon_l = \frac{1}{2}\left(\boldsymbol{r}'^{\mathrm{T}} \boldsymbol{r}' - 1\right), \quad \kappa = \left|\frac{\mathrm{d}^2 \boldsymbol{r}}{\mathrm{d}s^2}\right|, \tag{8}$$

where $\mathrm{d}s$ is the infinitesimal arc length of the beam, which can be expressed as

$$\mathrm{d}s = \sqrt{\boldsymbol{r}'^{\mathrm{T}} \boldsymbol{r}'} \mathrm{d}p. \tag{9}$$

In general case, the vector of the element elastic forces $\boldsymbol{Q}_e$ can be written as

$$\boldsymbol{Q}_e = \left(\frac{\partial E_p}{\partial \boldsymbol{e}}\right) = \int_0^l E A \varepsilon_l \frac{\partial \varepsilon_l}{\partial \boldsymbol{e}} \mathrm{d}p + \int_0^l E I \kappa \frac{\partial \kappa}{\partial \boldsymbol{e}} \mathrm{d}p = \boldsymbol{Q}_{el} + \boldsymbol{Q}_{ek} = \left[\boldsymbol{K}_l(\boldsymbol{e}) + \boldsymbol{K}_t(\boldsymbol{e})\right]\boldsymbol{e}, \tag{10}$$

where $\boldsymbol{Q}_{el}$ is element longitudinal elastic force, $\boldsymbol{Q}_{ek}$ is element transverse elastic force, $\boldsymbol{K}_l(\boldsymbol{e})$ is (nonlinear) longitudinal stiffness matrix and $\boldsymbol{K}_t(\boldsymbol{e})$ is (nonlinear) transverse stiffness matrix.

The way of the strain and curvature calculation can be simplified by several presuppositions of the way of the beam deformation. In Berzeri (2000) several suitable models for both longitudinal and transverse elastic forces are introduced.

The whole model of the ANCF element is of the form

$$\boldsymbol{M}_e\ddot{\boldsymbol{e}} + \boldsymbol{K}_e(\boldsymbol{e})\boldsymbol{e} = \boldsymbol{Q}_{ek} \tag{11}$$

and is characterized by constant mass matrix $\boldsymbol{M}_e$, strongly nonlinear stiffness matrix $\boldsymbol{K}_e(\boldsymbol{e}) = \boldsymbol{K}_l(\boldsymbol{e}) + \boldsymbol{K}_t(\boldsymbol{e})$ derived using the strain energy and by vector of external forces $\boldsymbol{Q}_{ek}$.

The assembling of a discretized flexible body model is straightforward and can be extended by a suitable model of viscous forces

$$\boldsymbol{M}\,\ddot{\boldsymbol{q}} + \boldsymbol{B}(\dot{\boldsymbol{q}}, \boldsymbol{q})\dot{\boldsymbol{q}} + \boldsymbol{K}(\boldsymbol{q})\boldsymbol{q} = \boldsymbol{Q}_k\,, \tag{12}$$

where $\boldsymbol{q}$ is the vector of all elastic coordinates of the flexible body and $\boldsymbol{B}$ is damping matrix. This model can be combined with models of other flexible or rigid bodies and with the model of kinematic joints.

ANALYTICAL APPROACH TO THE MODELLING OF THE CABLE MECHANISM DYNAMICS BASED ON HAMILTON'S PRINCIPLE

The basis of analytical approach to the modelling of the cable mechanism dynamics based on Hamilton's principle is given in Du (2015).

Part of the cable mechanics is depicted in Fig. 6.

Kinetic T_1 and potential V_1 energies of the pulley and the cable wound on it can be expressed in form (without subscript of *i*-th cable)

$$\begin{aligned} T_1 &= \int_0^{\xi} \frac{1}{2}\mu\,\dot{\boldsymbol{r}}^{\mathrm{T}}\dot{\boldsymbol{r}}\,\mathrm{d}s + \frac{1}{2}I_d\,\dot{\vartheta}^2 = \frac{1}{2}(\mu\,\xi + \kappa)\,\dot{\xi}^2\,, \quad s \in \langle 0, \xi \rangle, \quad I_d = \kappa\, d^2\,, \\ V_1 &= \int_0^{\xi/d} \mu\, g\, d\left(-\boldsymbol{r}_d^{\mathrm{T}}\boldsymbol{e}_3 + d\sin\varphi\right)d\varphi = -\mu\, g\, d\,\xi\,\boldsymbol{r}_d^{\mathrm{T}}\boldsymbol{e}_3 + \mu\, g\, d^2\left(1 - \cos\frac{\xi}{d}\right), \end{aligned} \tag{13}$$

where μ is mass per unit length of the cable, $\boldsymbol{e}_3$ is the unit vector in the direction of gravity, d is the radius of the pulley, g is the gravitational acceleration and position vectors $\boldsymbol{r}$ and $\boldsymbol{r}_d$ are evident from Fig. 6.

Kinetic T_2 and potential V_2 energies (gravitational and deformational) of the deployed cable can be expressed in form

$$\begin{aligned} T_2 &= \int_{\xi}^{s} \frac{1}{2}\mu\,\dot{\boldsymbol{r}}^{\mathrm{T}}\dot{\boldsymbol{r}}\,\mathrm{d}s\,, \\ V_2 &= \int_{\xi}^{L}\left(\frac{1}{2}EA\,\varepsilon^2 - \mu\, g\,\boldsymbol{r}_d^{\mathrm{T}}\boldsymbol{e}_3\right)\mathrm{d}s\,, \quad \varepsilon = \left|\boldsymbol{r}^{\backslash}\right| - 1, \quad \left|\boldsymbol{r}^{\backslash}\right| = \sqrt{\boldsymbol{r}^{\backslash\mathrm{T}}\boldsymbol{r}^{\backslash}}, \quad \boldsymbol{r}^{\backslash} = \frac{\partial \boldsymbol{r}}{\partial s}\,, \end{aligned} \tag{14}$$

where E is the Young modulus of the cable material and A is the cable cross section area.

If the end-effector is e.g. point mass, kinetic and potential energies of the end-effector take form

$$T_3 = \frac{1}{2} m\, \dot{\boldsymbol{r}}_L^{\mathrm{T}} \dot{\boldsymbol{r}}_L \ , \qquad V_3 = -m\, g\, \boldsymbol{r}_L^{\mathrm{T}} \boldsymbol{e}_3 \ , \tag{15}$$

where $\boldsymbol{r}_L$ is the position vector of the end-effector (identical with end point of each cable) and m is mass of the end-effector. In other cases the end points of cables will be coupled with coordinates of end-effector by means of kinematical boundary conditions.

For assemblage of equations of motion can be used Hamilton's principle in form

$$\delta \int_0^t \left[\sum_{i=1}^{N} \left(T_{1i} - V_{1i} + T_{2i} - V_{2i} \right) + T_3 - V_3 \right] \mathrm{d}t = 0 , \tag{16}$$

where t is time and subscripts i correspond to individual cables and pulleys.

Having performed the variation of Hamilton's functional it can be accessed to relation

$$\begin{aligned}
&-\sum_{i=1}^{N} \int_0^t \left\{ \frac{1}{2} \mu\, \dot{\xi}_i^2 + \left(\mu\, \xi_i + \kappa \right) \ddot{\xi}_i \right\} \delta\xi_i \ \mathrm{d}t + \sum_{i=1}^{N} \int_0^t \left\{ \frac{1}{2} \mu \left(\boldsymbol{r}_i^{\backslash \mathrm{T}} \boldsymbol{r}_i^{\backslash} \right) \dot{\xi}_i^2 \right\} \delta\xi_i \ \mathrm{d}t - \\
&-\sum_{i=1}^{N} \int_0^t \int_{\xi_i}^{L_i} \mu\, \ddot{\boldsymbol{r}}_i^{\mathrm{T}} \delta\boldsymbol{r}_i \ \mathrm{d}s\, \mathrm{d}t + \sum_{i=1}^{N} \mu\, g \int_0^t \left\{ \boldsymbol{r}_d^{\mathrm{T}} \boldsymbol{e}_3 - d \sin \frac{\xi_i}{d} \right\} \delta\xi_i \ \mathrm{d}t - \\
&-\sum_{i=1}^{N} \int_0^t \left\{ EA \frac{\left| \boldsymbol{r}_{L_i}^{\backslash} \right| - 1}{\left| \boldsymbol{r}_{L_i}^{\backslash} \right|} \boldsymbol{r}_{L_i}^{\backslash \mathrm{T}} \delta\boldsymbol{r}_{L_i} + EA \frac{\left| \boldsymbol{r}_{\xi_i}^{\backslash} \right| - 1}{\left| \boldsymbol{r}_{\xi_i}^{\backslash} \right|} \boldsymbol{r}_{\xi_i}^{\backslash \mathrm{T}} \boldsymbol{r}_{\xi_i}^{\backslash} \delta\xi_i \right\} \mathrm{d}t + \\
&+\sum_{i=1}^{N} \int_0^t \int_{\xi_i}^{L_i} \left\{ EA \frac{\left| \boldsymbol{r}_i^{\backslash} \right| - 1}{\left| \boldsymbol{r}_i^{\backslash} \right|} \boldsymbol{r}_i^{\backslash \mathrm{T}} \right\} \delta\boldsymbol{r}_i \ \mathrm{d}s\, \mathrm{d}t + \sum_{i=1}^{N} \int_0^t \int_{\xi_i}^{L_i} \mu\, g\, \delta\boldsymbol{r}_i^{\mathrm{T}} \boldsymbol{e}_3 \ \mathrm{d}s\, \mathrm{d}t + \\
&+\sum_{i=1}^{N} \int_0^t \left\{ \frac{1}{2} EA \left(\left| \boldsymbol{r}_{\xi_i}^{\backslash} \right| - 1 \right)^2 - \mu\, g\, \boldsymbol{r}_{\xi_i}^{\mathrm{T}} \boldsymbol{e}_3 \right\} \delta\xi_i \ \mathrm{d}t - \int_0^t m\, \ddot{\boldsymbol{r}}_L^{\mathrm{T}} \delta\boldsymbol{r}_L \mathrm{d}t + \int_0^t m\, \delta\boldsymbol{r}_L^{\mathrm{T}} \boldsymbol{e}_3 \mathrm{d}t + \\
&+\sum_{i=1}^{N} \int_0^t \frac{M_i}{d} \delta\xi_i \ \mathrm{d}t = 0 ,
\end{aligned} \tag{17}$$

where M_i is the driving torque acting on the i-th pulley, $\boldsymbol{r}_i = \boldsymbol{r}_i(s, \xi, t)$, $\left| \boldsymbol{r}_{L_i}^{\backslash} \right| = \sqrt{\boldsymbol{r}_{L_i}^{\backslash \mathrm{T}} \boldsymbol{r}_{L_i}^{\backslash}} = \sqrt{\frac{\partial \boldsymbol{r}_i^{\mathrm{T}}(L_i, \xi_i, t)}{\partial s} \frac{\partial \boldsymbol{r}_i(L_i, \xi_i, t)}{\partial s}}$, $\left| \boldsymbol{r}_{\xi_i}^{\backslash} \right| = \sqrt{\frac{\partial \boldsymbol{r}_i^{\mathrm{T}}(\xi_i, t)}{\partial s} \frac{\partial \boldsymbol{r}_i(\xi_i, t)}{\partial s}}$.

The terms staying at the independent variations $\delta\xi_i$, $\delta\boldsymbol{r}_i$ and $\delta\boldsymbol{r}_L$ have to be equal to zero and then it can be accessed to N scalar equations

$$-\left(\mu\, \xi_i + \kappa \right) \ddot{\xi}_i - \mu\, g\, d \sin \frac{\xi_i}{d} - EA\, H \left(\left| \boldsymbol{r}_{\xi_i}^{\backslash} \right| - 1 \right) \frac{\left| \boldsymbol{r}_{\xi_i}^{\backslash} \right| - 1}{\left| \boldsymbol{r}_{\xi_i}^{\backslash} \right|} \boldsymbol{r}_{\xi_i}^{\backslash \mathrm{T}} \boldsymbol{r}_{\xi_i}^{\backslash} + \frac{M_i}{d} = 0 , \tag{18}$$

to N vector equations ($3N$ scalar equations)

$$\ddot{\boldsymbol{r}}_i = \frac{EA}{\mu} H\left(\left|\boldsymbol{r}_i^{\backslash}\right| - 1\right)\left[\boldsymbol{r}_i^{\backslash\backslash} - \frac{\boldsymbol{r}_i^{\backslash\backslash}}{\left|\boldsymbol{r}_i^{\backslash}\right|} + \frac{\boldsymbol{r}_i^{\backslash\backslash\,\mathrm{T}}\boldsymbol{r}_i^{\backslash}}{\left|\boldsymbol{r}_i^{\backslash}\right|^3}\boldsymbol{r}_i^{\backslash}\right] + g\,\boldsymbol{e}_3 \tag{19}$$

and to 1 vector equation (3 scalar equations)

$$\ddot{\boldsymbol{r}}_L = \frac{EA}{m} H\left(\left|\boldsymbol{r}_{L_i}^{\backslash}\right| - 1\right)\frac{\left|\boldsymbol{r}_{L_i}^{\backslash}\right| - 1}{\left|\boldsymbol{r}_{L_i}^{\backslash}\right|}\boldsymbol{r}_{L_i}^{\backslash} + g\,\boldsymbol{e}_3\,, \tag{20}$$

where function $H(\ )$ represents Heaviside's step function respecting only positive stretching (pull deformations) of individual cables. The first (scalar) equation corresponds to the moment equilibrium condition of each pulley, the second (vector) equation describes the equilibrium of the infinitesimal element of the i-th cable. The third (vector) equation corresponds to the equilibrium of the point mass (end-effector). The last equations have to be supplemented by boundary conditions, which in this case take the form of N-1 vector equation

$$\ddot{\boldsymbol{r}}_L = \ddot{\boldsymbol{r}}_1(s_1, \xi_1, t) = \ddot{\boldsymbol{r}}_2(s_2, \xi_2, t) = \ldots = \ddot{\boldsymbol{r}}_N(s_N, \xi_N, t). \tag{21}$$

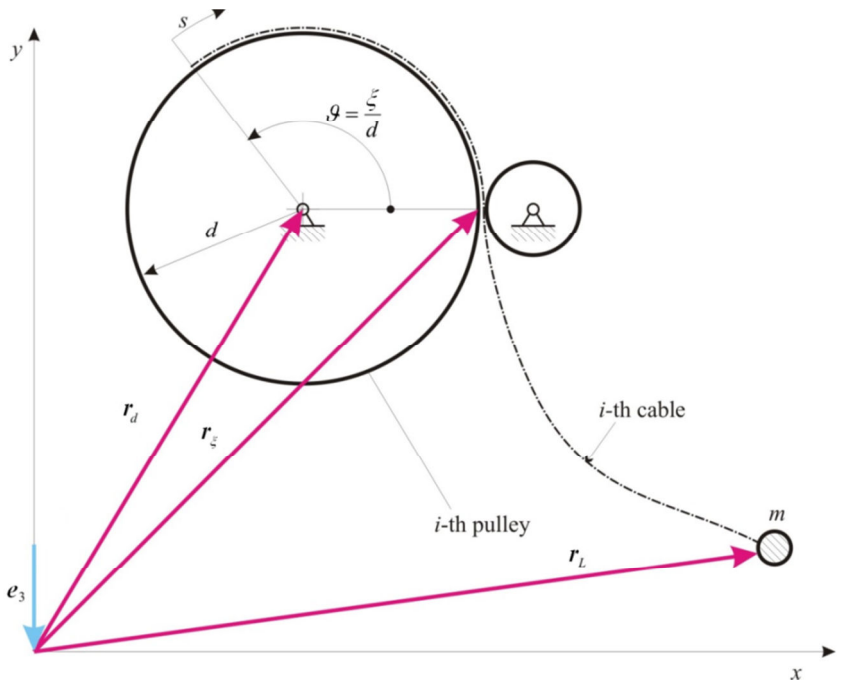

Fig. 6 - Part of the cable mechanism with pulley

Let's approximate the solution in form

$$\boldsymbol{r}_i(s, \xi_i, t) = \boldsymbol{r}_{\xi_i} + \boldsymbol{\Psi}_i(s, \xi_i)\,\boldsymbol{a}_i(t), \quad (\ )^{\backslash} = \frac{\partial}{\partial s}, \quad \boldsymbol{r}_{L_i} = \boldsymbol{r}_{L_i}(\xi_i, t) = \boldsymbol{r}_{\xi_i} + \boldsymbol{\Psi}_i(L_i, \xi_i)\,\boldsymbol{a}_i(t), \tag{22}$$

where $\boldsymbol{a}_i(t) \in \mathbf{R}^{3M,1}$ are unknown searched time functions,

$$\boldsymbol{\Psi}_i(s, \xi_i) = \begin{bmatrix} \boldsymbol{u}_i(s, \xi_i) & & \\ & \boldsymbol{u}_i(s, \xi_i) & \\ & & \boldsymbol{u}_i(s, \xi_i) \end{bmatrix} \in \mathbf{R}^{3,3M}, M = 6,$$

$$\boldsymbol{u}_i(s, \xi_i) = \left[\frac{s - \xi_i(t)}{L_i}, \left(\frac{s - \xi_i(t)}{L_i}\right)^2, \ldots, \left(\frac{s - \xi_i(t)}{L_i}\right)^6\right] \in \mathbf{R}^{1,6}.$$

When it is assumed that $\xi_i(t)$ are prescribed time functions Eq. (18) serves only for the determination of pulley torques. Remaining Eqs. (19) and (20) after substituting approximation take form of N vector equations

$$\begin{aligned}&\boldsymbol{\Psi}_i^{\backslash\backslash}\,\dot{\xi}_i^2\,\boldsymbol{a}_i-\boldsymbol{\Psi}_i^{\backslash}\,\ddot{\xi}_i\boldsymbol{a}_i-2\boldsymbol{\Psi}_i^{\backslash}\,\dot{\xi}_i\,\dot{\boldsymbol{a}}_i+\boldsymbol{\Psi}_i\,\ddot{\boldsymbol{a}}_i=\\&=\frac{EA}{\mu}\left\{\boldsymbol{\Psi}_i^{\backslash\backslash}\,\boldsymbol{a}_i-\frac{\boldsymbol{\Psi}_i^{\backslash\backslash}\,\boldsymbol{a}_i}{\sqrt{\boldsymbol{a}_i^{\mathrm{T}}\,\boldsymbol{\Psi}_i^{\backslash\mathrm{T}}\,\boldsymbol{\Psi}_i^{\backslash}\,\boldsymbol{a}_i}}+\frac{\left(\boldsymbol{a}_i^{\mathrm{T}}\,\boldsymbol{\Psi}_i^{\backslash\mathrm{T}}\,\boldsymbol{\Psi}_i^{\backslash}\,\boldsymbol{a}_i\right)\boldsymbol{\Psi}_i^{\backslash}\,\boldsymbol{a}_i}{\left(\boldsymbol{a}_i^{\mathrm{T}}\,\boldsymbol{\Psi}_i^{\backslash\mathrm{T}}\,\boldsymbol{\Psi}_i^{\backslash}\,\boldsymbol{a}_i\right)^{\frac{3}{2}}}\right\}+g\,\boldsymbol{e}_3\end{aligned}\tag{23}$$

and 1 vector equation (k is the subscript corresponding to the end point of one chosen k-th cable)

$$\boldsymbol{\Psi}_{kL}^{\backslash\backslash}\,\dot{\xi}_k^2\,\boldsymbol{a}_k-\boldsymbol{\Psi}_{kL}^{\backslash}\,\ddot{\xi}_k\,\boldsymbol{a}_k-2\boldsymbol{\Psi}_{kL}^{\backslash}\,\dot{\xi}_k\,\dot{\boldsymbol{a}}_k+\boldsymbol{\Psi}_{kL}\,\ddot{\boldsymbol{a}}_k=g\,\boldsymbol{e}_3-\frac{EA}{m}\sum_{i=1}^{N}\frac{\sqrt{\boldsymbol{a}_i^{\mathrm{T}}\,\boldsymbol{\Psi}_{iL}^{\backslash\mathrm{T}}\,\boldsymbol{\Psi}_{iL}^{\backslash}\,\boldsymbol{a}_i}-1}{\sqrt{\boldsymbol{a}_i^{\mathrm{T}}\,\boldsymbol{\Psi}_{iL}^{\backslash\mathrm{T}}\,\boldsymbol{\Psi}_{iL}^{\backslash}\,\boldsymbol{a}_i}}\boldsymbol{\Psi}_{iL}^{\backslash}\,\boldsymbol{a}_i\,.\tag{24}$$

Left hand side of Eq. (24) corresponds to the acceleration of mass point, which can be expressed as acceleration of end point of one chosen k-th cable. After approximation boundary conditions (21) have form

$$\begin{aligned}&\boldsymbol{\Psi}_{(i+1)L}^{\backslash\backslash}\,\dot{\xi}_{i+1}^2\,\boldsymbol{a}_{i+1}-\boldsymbol{\Psi}_{(i+1)L}^{\backslash}\,\ddot{\xi}_{i+1}\boldsymbol{a}_{i+1}-2\boldsymbol{\Psi}_{(i+1)L}^{\backslash}\,\dot{\xi}_{i+1}\,\dot{\boldsymbol{a}}_{i+1}+\boldsymbol{\Psi}_{(i+1)L}\,\ddot{\boldsymbol{a}}_{i+1}-\\&-\left(\boldsymbol{\Psi}_{iL}^{\backslash\backslash}\,\dot{\xi}_i^2\,\boldsymbol{a}_i-\boldsymbol{\Psi}_{iL}^{\backslash}\,\ddot{\xi}_i\boldsymbol{a}_i-2\boldsymbol{\Psi}_{iL}^{\backslash}\,\dot{\xi}_i\,\dot{\boldsymbol{a}}_i+\boldsymbol{\Psi}_{iL}\,\ddot{\boldsymbol{a}}_i\right)=\boldsymbol{0}\,,\quad i=1,2,\ldots,N-1\,.\end{aligned}\tag{25}$$

Using Galerkin's method for solving Eqs. (23), (24) and (25) each of Eqs. (23) is pre-multiplied by matrix $\widetilde{\boldsymbol{\Psi}}_i^{\mathrm{T}}$ and integrated from ξ_i to L_i,

where $\widetilde{\boldsymbol{\Psi}}_i(s,\xi_i)=\begin{bmatrix}\widetilde{\boldsymbol{u}}_i(s,\xi_i) & & \\ & \widetilde{\boldsymbol{u}}_i(s,\xi_i) & \\ & & \widetilde{\boldsymbol{u}}_i(s,\xi_i)\end{bmatrix}\in\mathbf{R}^{3,3(M-1)},\quad M=6\,,$

$$\widetilde{\boldsymbol{u}}_i(s,\xi_i)=\left[\frac{s-\xi_i(t)}{L_i},\left(\frac{s-\xi_i(t)}{L_i}\right)^2,\ldots,\left(\frac{s-\xi_i(t)}{L_i}\right)^5\right]\in\mathbf{R}^{1,5}.$$

Now it can be accessed to the total equation of motion in the form of

$$\boldsymbol{M}(t)\ddot{\boldsymbol{a}}(t)+\boldsymbol{B}(t)\dot{\boldsymbol{a}}(t)+\boldsymbol{K}(t)\boldsymbol{a}(t)=\boldsymbol{f}[\boldsymbol{a}(t)]\,,\tag{26}$$

$\boldsymbol{M}(t),\boldsymbol{B}(t),\boldsymbol{K}(t)\in\mathbf{R}^{3MN,\,3MN}$, $\boldsymbol{f}[\boldsymbol{a}(t)]\in\mathbf{R}^{3MN}$, which is the system of nonlinear ordinary differential equations, whose solution can be obtained using e.g. the Runge-Kutta method.

CONCLUSIONS

This paper summarizes the possible approaches suitable for the modelling of cable and fibre dynamics in the framework of various mechanical systems. Force representation of the cable, a point-mass model, absolute nodal coordinate formulation (ANCF) and a general model involving cables with distributed mass and time-varying length based on Hamilton's principle are introduced.

Future work will be focused on the implementation of the point-mass model of the cable and the modelling of its interaction with the pulley (the advantage of this approach is supposed to be in a precise physical interpretation of the problem and in a short computational time).

ACKNOWLEDGMENTS

The paper has originated in the framework of the institutional support for the long-time conception development of the research institution provided by the Ministry of Industry and Trade of the Czech Republic to Research and Testing Institute Plzeň and solving project of the Czech Science Foundation No. 15-20134S.

REFERENCES

[1]-Awrejcewicz J. Classical Mechanics: Dynamics. Springer, New York, 2012.

[2]-Berzeri M, Shabana AA. Development of simple models for the elastic force in the absolute nodal co-ordinate formulation. Journal of Sound and Vibrations, 2000, 235, p. 539-565.

[3]-Bulín R, Hajžman M, Polach P. Analysis of vibrations of a cable-pulley system using the absolute nodal coordinate formulation. In: Awrejcewicz J, Kaźmierczak M, Mrozowski J, Olejnik P (eds) Proceedings of 13th Conference on Dynamical Systems - Theory and Applications, Dynamical Systems - Mechatronics and Life Sciences, Łódź University of Technology, Łódź, 2015, p. 111-120.

[4]-Bulín R, Hajžman *et al*. Nonlinear dynamics of a cable-pulley system using the absolute nodal coordinate formulation. Mechanics Research Communications, 2017. (to appear)

[5]-Diao X, Ma O. Vibration Analysis of Cable-driven Parallel Manipulators. Multibody System Dynamics, 2009, 21, p. 347-360.

[6]-Du J, Agrawal SK. Dynamic modeling of cable-driven parallel manipulators with distributed mass flexible cables. Journal of Vibration and Acoustics, 2015, 137, p. 021020-1-021020-8.

[7]-Freire A, Negrão J. Nonlinear Dynamics of Highly Flexible Partially Collapsed Structures. In: Mota Soares CA, Martins JAC, Rodrigues HC, Ambrósio JAC, Pina CAB, Mota Soares CM, Pereira EBR, Folgado J (eds) Proceedings of III European Conference on Computational Mechanics, Solids, Structures and Coupled Problems in Engineering, Laboratório Nacional de Engenharia Civil, Lisbon, 2006, CD-ROM.

[8]-Gerstmayr J, Sugiyama H, Mikkola A. Developments and Future Outlook of the Absolute Nodal Coordinate Formulation. In: Eberhard P, Ziegler P (eds) Proceedings of The 2nd Joint International Conference on Multibody System Dynamics, University of Stuttgart, Stuttgart, 2012, USB flash drive.

[9]-Hajžman M, Bulín R, Polach P. Nonlinear analysis of the cable-pulley interaction. In: Font-Llagunes JM (ed) Proceedings of ECCOMAS Thematic Conference on Multibody Dynamics 2015, Universitat Politècnica de Catalunya, Barcelona, 2015, p. 554-564.

[10]-Hajžman M, Polach P. Modelling of Flexible Bodies in the Framework of Multibody Systems. In: Skočilasová B (ed) Proceedings of 6th International Conference Dynamics of Rigid and Deformable Bodies 2008, Jan Evangelista Purkyně University in Ústí nad Labem, Ústí nad Labem, 2008, p. 33-42.

[11]-Hajžman M, *et al.*Modelling of Cables for Application in Cable-based Manipulators Design. In: Samin J-C, Fisette P (eds) Proceedings of ECCOMAS Thematic Conference Multibody Dynamics 2011, Université catholique de Louvain, Brussels, 2011, USB flash drive.

[12]-Heyden T, Woernle C. Dynamics and Flatness-based Control of a Kinematically Undetermined Cable Suspension Manipulator. Multibody System Dynamics, 2006, 16, p. 155-177.

[13]-Kamman JW, Huston RL. Multibody Dynamics Modeling of Variable Length Cable Systems. Multibody System Dynamics, 2001, 5, p. 211-221.

[14]-Liu C, Tian Q, Hu H. New spatial curved beam and cylindrical shell elements of gradient-deficient Absolute Nodal Coordinate Formulation. Nonlinear Dynamics, 2012, 70, p. 1903-1918.

[15]-Lugrís U, Escalona J, Dopico D, Cuadrado J. Efficient and Accurate Simulation of the Rope-sheave Interaction in Weight-lifting Machines. Proceedings of the Institution of Mechanical Engineers, Part K: Journal of Multi-body Dynamics, 2011, 225, p. 331-343.

[16]-Ottaviano E, Gattulli V, Potenza F, Rea P. Modeling a Planar Point Mass Sagged Cable-Suspended Manipulator. In: Chang S-H, Ceccarelli M, Sung C-K, Chang J-Y, Liu T (eds) Proceedings of 14th IFToMM World Congress. Chinese Society of Mechanism and Machine Theory, Taipei, 2015, 4, p. 2696-2702.

[17]-Polach P, *et al.*, Alternative modelling of cables of varying length. In: Adámek V, Zajíček M, Jonášová A (eds) Proceedings of 31st Conference with International Participation Computational Mechanics 2015, Univ. of West Bohemia in Plzeň, Špičák, 2015a, p. 91-92.

[18]-Polach P, Hajžman M, Václavík J. Experimental and Computational Investigation of a Simple Mechanical System with Fibre. Engineering Mechanics, 2014, 21, p. 19-27.

[19]-Polach P, Hajžman M. Influence of the fibre spring-damper model in a simple laboratory mechanical system on the coincidence with the experimental results. In: Font-Llagunes JM (ed) ECCOMAS Thematic Conference on Multibody Dynamics 2015. Universitat Politècnica de Catalunya, Barcelona, 2015b, p. 356-365.

[20]-Schiehlen W. Research Trends in Multibody System Dynamics. Multibody System Dynamics, 2007, 18, p. 3-13.

[21]-Shabana AA. Flexible Multibody Dynamics: Review of Past and Recent Developments. Multibody System Dynamics, 1997, 1, p. 189-222.

[22]-Shabana AA. Dynamics of Multibody Systems, Third Edition. Cambridge University Press, Cambridge, 2005.

[23]-Stejskal V, Valášek M. Kinematics and Dynamics of Machinery. Marcel Dekker, Inc., New York, 1996.

[24]-Wasfy TM, Noor AK. Computational Strategies for Flexible Multibody Systems. Applied Mechanics Review, 2003, 56, p. 553-613.

[25]-Wittbrodt E, Adamiec-Wójcik I, Wojciech S. Dynamics of Flexible Multibody Systems, Rigid Finite Element Method. Springer, Berlin, 2006.

[26]-Zi B, Duan BY, Du JL, Bao H. Dynamic Modeling and Active Control of a Cable-suspended Parallel Robot. Mechatronics, 2008, 18, p. 1-12.